Biochem Genet (2013) 51:119–130
DOI 10.1007/s10528-012-9547-8

The *Igf2as* Transcript is Exported into Cytoplasm and Associated with Polysomes

Carolina Duart-Garcia · Martin H. Braunschweig

Received: 3 November 2011 / Accepted: 12 September 2012 / Published online: 30 October 2012

Abstract Murine insulin-like growth factor 2 antisense (*Igf2as*) transcripts originate from the opposite strand of the same *Igf2* locus as the *Igf2* sense mRNA. The *Igf2*, insulin 2 (*Ins2*), and *H19* genes form a cluster of imprinted genes on chromosome 7. Loss of imprinting of *IGF2* in humans is associated with Beckwith–Wiedemann syndrome and Silver–Russell syndrome, as well as with Wilm's tumor and colorectal cancer. We developed a RNA-FISH protocol to detect *Igf2as* and *Igf2* transcripts. The results from the RNA-FISH were confirmed with quantitative real-time PCR and clearly indicate that the *Igf2as* transcripts are predominantly located in the cytoplasm of C2C12 cells. In a polysome association study, we showed that the *Igf2as* sedimented with polysomes in a sucrose gradient. The cellular localization of *Igf2as* transcripts together with polysome fractionation analysis provides compelling evidence that the *Igf2as* is protein coding.

Keywords *Igf2as* · RNA-FISH · C2C12 cells · Genomic imprinting · Polysome analysis

Introduction

Genomic imprinting is a phenomenon resulting in a parent-of-origin specific gene expression (Reik and Walter 2001). Imprinted genes are controlled by imprinting control regions (ICRs) as well as cis-acting long noncoding RNA such as *Xist, Kcnq1ot1*, and *Air* (Bartolomei and Ferguson-Smith 2011; Mohammad et al. 2009). The ICRs carry parental specific epigenetic modifications including DNA methylation that are acquired during primordial germ cell development and

C. Duart-Garcia · M. H. Braunschweig (✉)
Institute of Genetics, Vetsuisse Faculty, University of Bern, Bremgartenstrasse 109a, 3001 Berne, Switzerland
e-mail: martin.braunschweig@vetsuisse.unibe.ch

maintained after fertilization (Pauler et al. 2007). The insulin-like growth factor 2 gene (*Igf2*) encodes for the insulin-like growth factor-II peptide, a growth factor with a principal function in myogenesis (Florini et al. 1991, 1996). The Igf2 peptide is a member of the insulin-like growth factor (IGF) family. IGFs stimulate many anabolic responses in myoblasts and stimulate both proliferation and differentiation of the myoblasts (Florini et al. 1996). The *Igf2* gene was one of the first genes reported to be imprinted. Only the paternal allele of *Igf2* is expressed, leading to functional hemizygosity. This was proven by generating chimeric mice that had one of the *Igf2* alleles disrupted. Heterozygous offspring from male *Igf2* mutant mice were 60 % smaller than the wildtype mice, demonstrating the importance of *Igf2* for embryonic and fetal growth (De Chiara et al. 1990, 1991). *Igf2*, insulin 2 (*Ins2*), and *H19* are located in a gene cluster that maps to the distal region of mouse chromosome 7 (Monk et al. 2006). *H19* is maternally expressed, whereas *Igf2* and *Ins2* are paternally expressed. An ICR about 2 kb upstream of *H19* is involved in the control of these reciprocally imprinted genes. This ICR is methylated on the paternal allele, which impairs the binding of the CCCTC-binding factor (CTCF or 11-zinc finger protein), leading to paternal *Igf2* expression. On the maternal chromosome, CTCF binds to the unmethylated ICR, which functions as an insulator blocking the interaction between *Igf2* promoters and enhancers downstream of *H19* (Bell and Felsenfeld 2000; Hark et al. 2000).

The first *IGF2AS* transcript was found in chicken embryo while studying *IGF2* expression (Taylor et al. 1991). This *IGF2AS* transcript overlapped *IGF2* in the second coding exon. Taylor et al. (1991) suggested that this antisense transcript may be responsible for low amounts of *IGF2* transcripts in embryos, considering the high expression level of *IGF2* transcript after birth. Later, Rivkin et al. (1993) reported the first *Igf2as* transcripts in mice. A detailed study revealed multiple *Igf2* sense and antisense transcripts including differential DNA methylation and tandem repeats at the mouse *Igf2* locus (Moore et al. 1997). No open reading frame could be identified in these antisense transcripts, and their function remains elusive.

The *IGF2* imprinted locus is still intensively studied, since it is implicated in Beckwith–Wiedemann syndrome and Silver–Russell syndrome, as well as in Wilm's tumor and colorectal cancer (Okutsu et al. 2000; Reik and Walter 2001; Monk et al. 2006; Berteaux et al. 2008). In this study, we investigated the localization of *Igf2as* transcripts in C2C12 myoblast cells relative to *Igf2* sense transcripts, and subsequently we performed a polysome association study. We report here for the first time that the *Igf2as* transcripts are present in the cytoplasm and are located in RNA-associated polysome fractions from C2C12 myoblast cells, suggesting that these transcripts are protein coding.

Materials and Methods

Cell Culture

C2C12 muscle myoblast cells from *Mus musculus* (American Type Culture Collection) were grown in Dulbecco's Modified Eagle's Medium supplemented

with 10 % fetal calf serum and penicillin–streptomycin solution to a final concentration of 1 %. The cells were incubated at 37 °C in a 5 % CO_2 atmosphere and were subcultured every 2 days with new medium. The procedure for subculturing C2C12 cells was as follows: discarding of old culture medium, washing with phosphate buffered saline (PBS), addition of 2 ml 5× trypsin–EDTA solution, and incubation at 37 °C until the cells were detached from the bottom of the flask (about 5 min). Fresh growth medium (at 37 °C) was then added to these cells, and approximately 1.5×10^5–1×10^6 C2C12 cells were transferred to a new flask and completed with growth medium to 10 ml.

RNA-FISH

Total RNA was isolated using Trizol reagent according to the manufacturer's instructions (Invitrogen) and treated with DNaseI (Ambion). RNA was then cleaned up with an RNeasy Mini Kit (Qiagen). The reverse transcription of RNA was performed with a First-Strand cDNA Synthesis Kit (GE Healthcare). The sequences of the RNA-FISH probes were selected following the recommendations of Arvey et al. (2010). The mouse *Igf2as* transcript sequence (accession no. NR_002855.2) was analyzed for repetitive elements using the Repeatmap program (http://cbio.mskcc.org/~aarvey/repeatmap/). A sequence of about 500 bp was then chosen to design a primer pair (http://frodo.wi.mit.edu/primer3; Table 1). The probe sequence to detect *Igf2* transcripts was selected from the coding sequence that is common for all known transcript variants (NM_010514.3). Locations of probes are shown in Fig. 1.

For the probe construction, the respective fragments for *Igf2* and *Igf2as* were PCR amplified using cDNA from C2C12 cells. The PCR products were subsequently cloned into pCRII-TOPO vectors according to the manufacturer's instructions (Invitrogen). Chemically competent cells were transformed and incubated overnight on agar plates. White colonies were then picked for further

Table 1 Primer pairs used to amplify the sequences for RNA-FISH probes and qPCR

Primer	Forward sequence	Reverse sequence	Product size (bp)
Igf2 antisense	5′GTTTGCAGAGTGCACACAA AGTGG3′	5′CCTGGCAAAGTCCAGGAG TTCATCT3′	350
Igf2 sense	5′TGGGCAAGTTCTTCCAATAT GACACC3′	5′TCTTAGTGTGGGACGTGAT GGAACTG3′	305
Igf2_negative	5′TGGGCAAGTTCTTCCAATA TGACACC3′	5′TCTTAGTGTGGGACGTGAT GGAACTG3′	305
Sense-Igf2_f/r	5′TGGGCAAGTTCTTCCAATA TG3′	5′CTTTGAGCTCTTTGGCAA GC3′	114
Igf2as_f/r	5′CACCAACATGAGGATTGC AC3′	5′AGGTCAGACAGCTCCAGA GG3′	99
Xist_f/r	5′ACAGCAGTTCTCCCAGCA TT3′	5′CCAGGCAATCCTTCTTCT TG3′	188

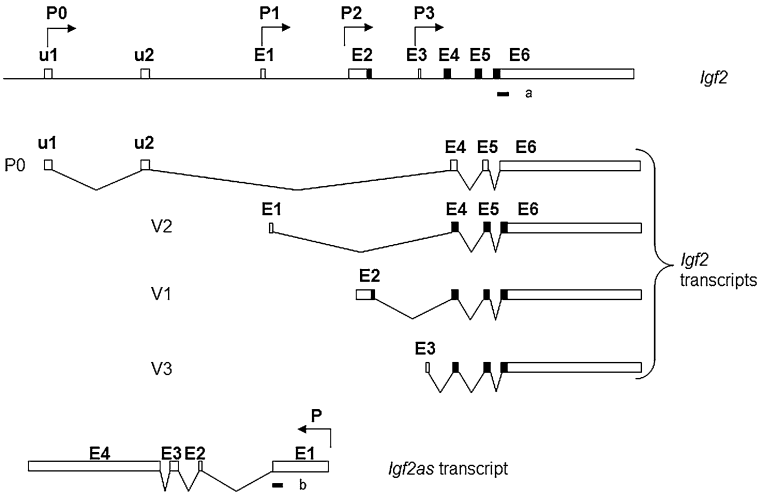

Fig. 1 Structure of the mouse *Igf2* gene and the region coding for *Igf2* antisense transcripts. *Arrows* indicate the four promoters (P0, P1, P2, and P3) for the *Igf2* gene and the promoter (P) for the *Igf2* antisense transcript. Eight exons are indicated in the *Igf2* gene, and four exons are shown in the *Igf2* antisense transcript. V1, V2, and V3 indicate the three transcript variants of the *Igf2* sense transcripts. Coding exons are shown in *black*. The FISH probes are labeled with lowercase "a" (for *Igf2*) and lowercase "b" (for *Igf2as*)

inspections. Plasmids were extracted with the QIAprep Spin Miniprep Kit according to the manufacturer's recommendation (Qiagen). Plasmids were Sanger-sequenced using the BigDye Terminator v3.1 Ready Reaction Cycle Sequencing kit and run on the ABI 3730 capillary sequencer (Applied Biosystems).

Circular plasmid DNA was opened with restriction endonucleases *Not*I (New England Biolabs). The digested plasmids were extracted with phenol–chloroform and precipitated with ethanol, and the concentration was measured with the NanoDrop ND-1000 Instrument (NanoDrop Technologies).

The in vitro transcription reaction used 1 μg of plasmid DNA for each Igf2as, Igf2, and negative Igf2 control probe to synthesize the corresponding labeled RNA-FISH probe. The in vitro transcription was performed with a Maxiscript kit (Ambion) using digoxigenin (DIG) RNA labeling mix (Roche) according to the manufacturer's protocol. The RNA-labeled probes were DNase digested to remove plasmid DNA and subsequently cleaned using the RNeasy Mini Kit (Qiagen).

RNA-FISH Procedure

C2C12 cells were grown on glass coverslips coated with poly-L-lysine to reach 90–95 % confluence. The cells were fixed with 4 % paraformaldehyde in PBS at room temperature for 20 min, then digested with 0.1 % Proteinase K (Sigma) in 5 % Tris–HCl and 1.5 % $CaCl_2$ preheated buffer (37 °C) for 5 min at 37 °C. After digestion, the cells were again fixed for 5 min in 4 % paraformaldehyde and subsequently washed at room temperature for 2 min in 2× SSC buffer.

Once the cells were fixed, they were incubated with prehybridization buffer containing 50 % formamide, 5× SSC, and 0.1 % Tween-20, during 1 h at 50 °C. The cells were then hybridized with prehybridization buffer containing 100 μg/ml fragmented salmon sperm DNA and 50 μg/ml heparin (Sigma) and using 1 μg/ml of the labeled probe. After the RNA probes were added, the probe mixture was heated to 80–85 °C for 2–3 min and then chilled on ice. After the hybridization mix was added to the fixed cells, the coverslips were covered with Gel Bond film (Bioproducts), sealed with rubber cement (Starkey), and incubated overnight at 50 °C.

The slides were washed with prehybridization buffer that was preheated to 55 °C and incubated at 55 °C for 1 h. A second wash at room temperature was made with 50 % PBT (1× PBS, 0.1 % Tween-20) and 50 % hybridization solution for 10 min, followed by a PBT washing step for 15 min. The fixed cells on the coverslips were blocked with western blocking reagent diluted 1:4 in PBT (Roche) for 30 min. The primary sheep anti-DIG antibody (Roche) stock solution was centrifuged at 500×*g* before use and diluted in western blocking reagent-PBT to 1:200. The cells were then incubated with this primary antibody for 1.5 h at room temperature. The slides were washed two times for 15 min in PBT and again incubated in western blocking reagent diluted 1:4 in PBT for 30 min. The stock solution of Alexa 555 donkey anti-sheep secondary antibody (Invitrogen) was also centrifuged briefly and then diluted in 1:4 blocking reagent-PBT solution in the ratio of 1:300. The slides were subsequently incubated with the diluted secondary antibody for 1 h at room temperature. Because of the light sensitivity of Alexa 555, the slides were thereafter protected from light. The slides were washed four times using PBT for 15 min. The nuclei were stained with TOTO3 (Invitrogen) for 30 min at room temperature and rinsed twice with PBT. The coverslips with the cells were mounted in prewarmed (50 °C) Glicergel (Dako) on new slides.

Fluorescent signals were visualized using an Olympus Fluoview FV1000 microscope with epifluorescence. Pictures were taken and analyzed using the FV10-ASW 1.7 Viewer software. They were further processed using Corel Photo-Paint ×4 software.

Quantification of RNA in Nucleus and Cytoplasm

RNA was extracted from both nuclear and cytoplasmic fractions using the Paris Kit according to the manufacturer's instructions, following the preparation of separate nuclear and cytoplasmic lysate protocol (Ambion).

RNA was DNase digested and cleaned up with the RNeasy Mini Kit (Qiagen). From the cleaned RNA fractions, cDNA was synthesized using a Quanti Tect Reverse Transcription kit, according to the manufacturer's protocol (Qiagen). For the cDNA synthesis, the same amount of RNA was used for both nuclear and cytoplasmic fractions, and 600 ng of nuclear and 600 ng of cytoplasmic RNA were reverse transcribed for each experiment.

The expression levels of *Igf2* and *Igf2as* transcripts in the nuclear and cytoplasmic fractions of C2C12 were quantified by qPCR using Power SYBR Green (Applied Biosystems). The expression levels were compared with two

endogenous controls, *Gapdh* (accession no. NM_008084.2) in the cytoplasm and *Xist* (accession no. NR_001570.2) in the nucleus. The primer sequences and product sizes for quantitative SYBR Green qPCR are given in Table 1.

In the quantitative SYBR Green qPCR, the expression levels of *Igf2* sense, *Gapdh*, and *Xist* were measured using 2 µl cDNA, and *Igf2as* transcripts used 5 µl. The reaction was run on the 7300 Real-Time PCR System (Applied Biosystems). RNA samples from three independent fractionations of nuclear and cytoplasmic fractions were quantified by qPCR in triplicate. Data were analyzed using the SDS version 1.3.1 software, according to the guidelines from Applied Biosystems. In the graph, the results are expressed as relative amounts of transcripts, which corresponds to the cycle threshold (Ct) values corrected for the RNA amounts used to synthesize the cDNA.

Polysome Fractionation

C2C12 cells were grown in 75 cm^2 dishes to 70 % confluence. One dish was treated with 100 µg/ml cycloheximide (Sigma) 3 min before harvest. A negative control plate remained without the cycloheximide treatment. The medium was then removed, and the cells were washed with cold PBS with 100 µg/ml cycloheximide and without it for the negative control. The cells treated with cycloheximide were harvested with 500 µl polysome buffer containing 140 mM NaCl, 1.5 mM $MgCl_2$, 10 mM Tris–HCl (pH 8), 0.5 % Nonidet P-40 (Roche), and RNasin (500 U/ml) on ice. The negative control cells were harvested using 400 µl of a buffer with the same composition but with 0.2 mM $MgCl_2$. The cells were then passed through a syringe and centrifuged at 14,000 rpm for 5 min at 4 °C to pellet the nuclei. The supernatant was collected and supplemented with 665 µg/ml heparin, 20 mM dithiothreitol, and 1 mM phenylmethanesulfonyl fluoride, including 100 µg/ml cycloheximide for the treated cells. The samples were then centrifuged at 14,000 rpm for 5 min at 4 °C to pellet the mitochondria and membrane debris. After centrifugation, 100 µl of 0.5 M EDTA was exclusively added to the 400 µl supernatant of the negative control cells. The mixture was loaded on top of a 7–47 % sucrose gradient and ultracentrifuged at 38,000 rpm for 2 h at 4 °C in a Sorvall TH-641 rotor (Kendro). From the gradients, 10 fractions of 1 ml were collected by puncturing the bottom of the tube. The samples were deproteinated by adding 100 µg/ml of Proteinase K, 1 % SDS, and 10 mM EDTA. The samples were extracted with phenol–chloroform and precipitated with ethanol. An RNA aliquot (3 µl) of each polysome fraction and the EDTA-disrupted negative control fraction was analyzed on 1.2 % agarose gel. The remaining 12 µl of RNA was used for cDNA synthesis with the First-strand cDNA Synthesis Kit (GE Healthcare), following the manufacturer's instructions. Quantification in duplicate of *Igf2as* and *Gapdh* transcript levels was performed by qPCR using TaqMan probes from Applied Biosystems (Table 2). For the quantification of *Igf2as,* a nested PCR procedure was applied by amplifying an *Igf2as* fragment for 10 cycles with Igf2as_outer primers followed by qPCR using Igf2as_inner primers and an Igf2as MGB probe (Table 2). The data were further analyzed.

Table 2 Primer pairs and probes used in TaqMan qPCR experiments

Primer	Forward sequence	Reverse sequence	Probe	Product size (bp)
Igf2as_ outer_f/r	5′CCACATAGGGACTC CACACC3′	5′AGGTCAGAC AGCTCCAGAGG3′		181
Igf2as TaqMan_f/r	5′TGCACCAAA CTGATCAACACAA3′	5′AAAGGCA GGGTTCCAGATGA3′	5′CACACCAAAA ATTCTTTC3′	63
Gapdh TaqMan_f/r	5′CGGCCGCA TCTTCTTGTG3′	5′TACGGCCAAA TCCGTTCAC3′	5′AGTGCCAGCC TCGTCCC GTAGACA3′	79

Results

Visualization of *Igf2as* Transcripts in C2C12 Cells

First we aimed to determine the subcellular localization of the *Igf2/Igf2as* sense and antisense pair in C2C12 murine myoblast cells, with the ultimate goal of establishing a function for *Igf2as*. We performed RNA-FISH and found that the *Igf2as* transcripts are predominantly located in the cytoplasm of C2C12 cells (Fig. 2). Fluorescence signals were evenly distributed in the cytoplasmic compartment of all cells, but many fewer fluorescence signals were observed in the nuclei (stained in blue). The analysis of hundreds of cells clearly suggests that the *Igf2as* transcripts are exported into the cytoplasm. In parallel, *Igf2* sense transcripts were also detected in RNA-FISH experiments. Strong fluorescence signals were homogeneously distributed in the cytoplasmic fraction of *Igf2*-probed C2C12 cells (Fig. 2). In all RNA-FISH experiments, a sense probe to *Igf2* transcripts was routinely included as a negative control probe. The fluorescence signals observed in the RNA-FISH experiments with the negative nontarget Igf2 control probe were very low and randomly distributed over the entire cells. Taken together, *Igf2as* is present in the cytoplasmic compartment of C2C12 cells. The intensity of the signals further showed that the *Igf2* sense transcript is much more abundant than the *Igf2as* transcript (Fig. 2).

Quantification of Transcripts in Nuclear and Cytoplasmic Fractions by qPCR

In order to confirm our RNA-FISH results and to quantify RNA transcripts in C2C12 cell fractions, we performed qPCR analysis. We separated the nuclear and cytoplasmic fractions from C2C12 cells and measured the amount of *Igf2* antisense transcripts in the nucleus and cytoplasm. Glyceraldehyde-3-phosphate dehydrogenase (*Gapdh*) and X-inactive specific transcript (*Xist*) were used as endogenous controls in the cytoplasmic and nuclear fractions, respectively. The level of expression is represented as relative amount of transcripts (Fig. 3). Similar to RNA-FISH, the qPCR analysis showed that the *Igf2as* expression was higher in the cytoplasmic fraction than in the nuclear fraction of C2C12 cells. *Igf2* sense

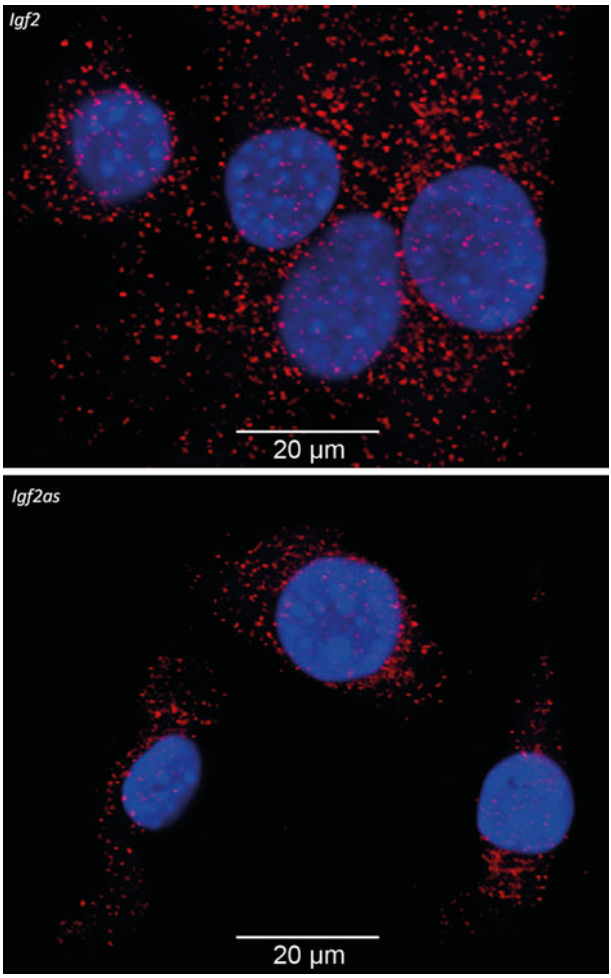

Fig. 2 RNA-FISH to detect *Igf2* and *Igf2as* transcripts in C2C12 cells. (*Top*) The *Igf2* probe hybridized against *Igf2* sense transcripts in C2C12 cells. (*Bottom*) The *Igf2as* probes hybridized against *Igf2* antisense transcripts in C2C12 cells. Fluorescent signals from the probes are shown as *red* flecks. The nuclei are stained with TOTO3 and shown as large *blue* round objects (Color figure online)

transcripts were more abundant in the cytoplasm than in the nuclear fraction. As expected, the *Gapdh* transcript level was higher in the cytoplasmic fraction. *Xist* transcripts appear to be predominantly located in the nuclear compartment.

Polysome Association Analysis

In order to determine whether *Igf2as* transcripts are protein coding, we performed a polysome association analysis. A positive association indicates translation of the transcripts. In this assay, we treated the cells with cycloheximide, which keeps the

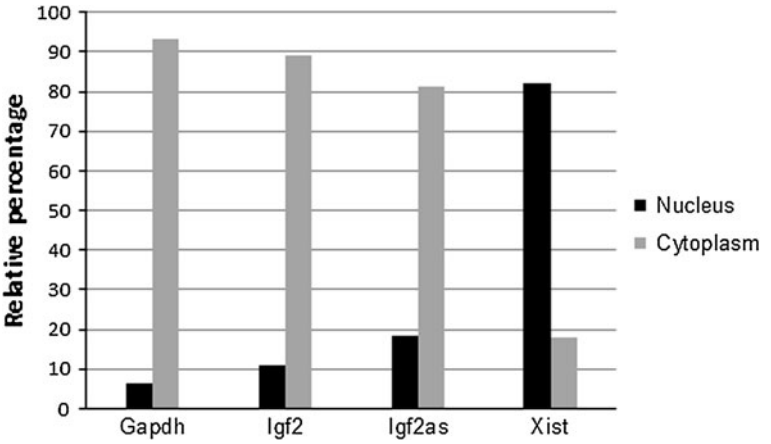

Fig. 3 Quantification of *Igf2as* transcripts compared with *Gapdh*, *Igf2*, and *Xist* expression. The results are expressed as relative amounts of transcripts. *Black bars* Nuclear fractions of C2C12 cells. *Gray bars* Cytoplasmic fractions of C2C12 cells. *Bars* represent the mean of three replicates of one experiment

translating RNA bound to the polysomes. Following the treatment, we purified RNA-associated polysomes by sucrose gradient differential centrifugation from C2C12 cells. We included a negative control containing an EDTA-treated C2C12 lysate, which disrupts the polysomes and impairs their location in the lower fractions of the gradient. In this way, the RNA associated with the polysomes is shifted to the upper fractions; RNAs associated with other proteins will not be affected. From each sucrose gradient, 10 fractions were collected. To control the experiment and observe the polysome location throughout the fractions, we visualized the 28S and 18S rRNAs in an agarose gel (Fig. 4). The gel showed the distribution of 28S and 18S rRNA from fractions 1–6, representing the polysomal fractions. Fractions 7–10 are frequently referred to as free RNA fractions. Fractions 1–4 from the negative control experiment were free of 28S and 18S rRNA, indicating disruption of polysomes by EDTA. *Igf2as* transcripts were detected in the polysomal fractions in the cycloheximide-treated cells (Fig. 5). In contrast, the transcript distribution in the EDTA-treated control experiment was shifted to the upper fractions, as expected for polysome-associated transcripts. This clearly indicates that the *Igf2as* transcripts are bound to polysomes and released from them by EDTA. Similarly, *Gapdh* control transcripts were present in the polysomal fractions and underwent a distribution shift after EDTA treatment (Fig. 5).

Discussion

We found significant expression levels of *Igf2as* transcripts in the cytoplasm of undifferentiated C2C12 cells by means of two independent analyses, RNA-FISH and cell fractionation followed by qPCR. The results strongly indicate that the *Igf2*as transcripts are functional rather than solely representing transcriptional noise.

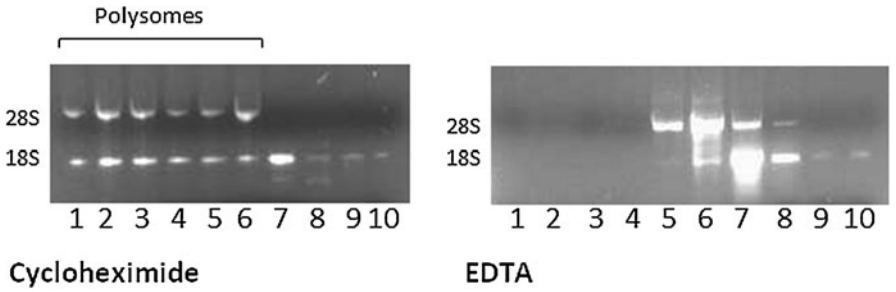

Fig. 4 Distribution of ribosomal RNA along the sucrose gradient. The C2C12 cells were treated with cycloheximide (*left*) or EDTA (*right*) and sedimented in a gradient of 7–47 % sucrose. The gradient was collected from the highest sucrose percentage (*lane 1*) to the lowest sucrose percentage (*lane 10*). In the cycloheximide treatment, the polysomal fractions are seen in *lanes 1–6*. In the EDTA treatment, the absence of 28S and 18S rRNA in those lanes indicates that the polysomes were disrupted and the ribosomes were shifted to the upper fractions

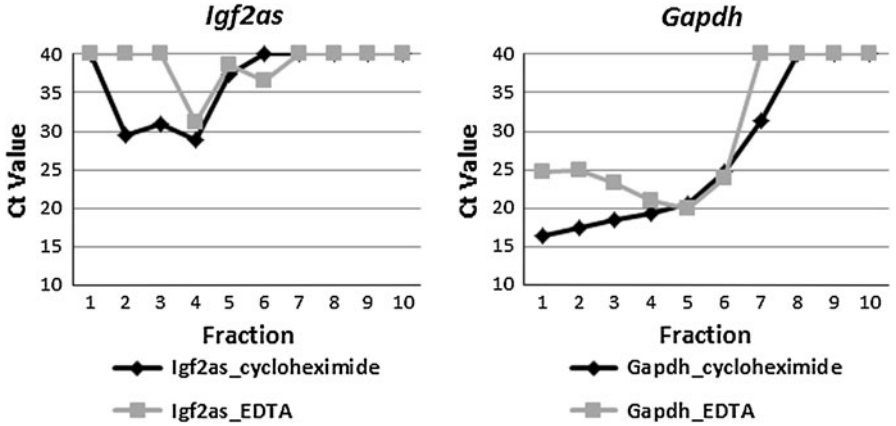

Fig. 5 Distribution of *Igf2as* and *Gapdh* transcripts along the fractions. The *Igf2* antisense (*left*) and *Gapdh* (*right*) transcripts were quantified by qPCR for each fraction (1–10). The Ct values plotted for *Igf2as* and *Gapdh* compare the cycloheximide (*black*) and EDTA (*gray*) experiments. The release of transcripts from the polysomes is reflected in the higher Ct values found for the EDTA-treated C2C12 cell lysate. A Ct value of 40 corresponds to "no amplification"

Additionally, the polysome study demonstrates that the *Igf2as* transcripts are associated with the polysomal fraction, strongly suggesting a protein coding function of *Igf2as*. A recent study performing ribosome profiling provides further evidence that the *Igf2as* sequences were found in ribosomes (Ingolia et al. 2011). An in silico analysis of their data on ribosome footprints converted to DNA revealed numerous 40 bp reads that map to the *Igf2as* sequence. We cannot exclude, however, that the *Igf2as* transcripts have further functions besides coding for proteins.

It is interesting that we found abundant fluorescence signals with the respective Igf2 sense and antisense probes in all C2C12 cells for each RNA-FISH experiment, which suggests co-expression of this sense/antisense pair in single cells.

Co-expression of the *Igf2/Igf2as* pair would allow these two transcripts to form RNA duplexes around exon 1 of *Igf2* variant 2 and around u1 of the placenta-specific transcript from promoter P0 (Fig. 1). The formation of duplexes between *Igf2as* and *Igf2* may lead to the masking of key regulatory features within either transcript, inhibiting the access and binding of important *trans*-acting factors (Beiter et al. 2009; Lavorgna et al. 2004). These RNA duplexes could also enter the RNA interference pathway and direct specific destruction of target mRNAs (Wang and Carmichael 2004; Kent and MacMillan 2004). Presently, we also cannot exclude that the *Igf2as* could code for a miRNA, since it has previously been reported that the *H19* transcript is processed into a primary miRNA transcript in both humans and mice (Cai and Cullen 2007). Alternatively, cytoplasmic long noncoding RNAs such as this *Igf2as* transcript can down-regulate the mRNA target by recruiting RNA decay proteins (Wang and Chang 2011).

In conclusion, our results clearly showed that the *Igf2as* transcripts are present in the cytoplasm and are associated with the polysome fractions. These results strongly indicate that the *Igf2as* is protein coding, although noncoding *Igf2as* functions are not yet formally excluded.

Acknowledgments The authors thank Philippe Plattet for technical advice and Tosso Leeb for scientific suggestions. This research was supported by the Swiss National Foundation (Project 31003A_127564).

References

Arvey A, Hermann A, Hsia CC, Ie E, Freund Y, McGinnis W (2010) Minimizing off-target signals in RNA fluorescent in situ hybridization. Nucleic Acids Res 38:e115

Bartolomei MS, Ferguson-Smith AC (2011) Mammalian genomic imprinting. Cold Spring Harb Perspect Biol 3:a002592

Beiter T, Reich E, Williams RW, Simon P (2009) Antisense transcription: a critical look in both directions. Cell Mol Life Sci 66:94–112

Bell AC, Felsenfeld G (2000) Methylation of a CTCF-dependent boundary controls imprinted expression of the *Igf2* gene. Nature 405:482–485

Berteaux N, Aptel N, Cathala G, Genton C, Coll J, Daccache A, Spruyt N, Hondermarck H, Dugimont T, Curgy JJ, Forné T, Adriaenssens E (2008) A novel *H19* antisense RNA overexpressed in breast cancer contributes to paternal *IGF2* expression. Mol Cell Biol 28:6731–6745

Cai X, Cullen BR (2007) The imprinted *H19* noncoding RNA is a primary microRNA precursor. RNA 13:313–316

De Chiara TM, Eftratiadis A, Robertson EJ (1990) A growth-deficiency phenotype in heterozygous mice carrying an insulin-like growth factor II gene disrupted by targeting. Nature 345:78–80

De Chiara TM, Robertson EJ, Efstratiadis A (1991) Parental imprinting of the mouse insulin-like growth factor II gene. Cell 64:849–859

Florini JR, Magri KA, Ewton DZ, James PL, Grindstaff K, Rotwein PS (1991) Spontaneous differentiation of skeletal myoblasts is dependent upon autocrine secretion of insulin-like growth factor-II. J Biol Chem 266:15917–15923

Florini JR, Ewton DZ, Coolican SA (1996) Growth hormone and the insulin-like growth factor system in myogenesis. Endocr Rev 17:481–517

Hark AT, Schoenherr CJ, Katz DJ, Ingram RS, Levorse JM, Tilghman SM (2000) CTCF mediates methylation-sensitive enhancer blocking activity at the *H19/Igf2* locus. Nature 405:486–489

Ingolia NT, Lareau LF, Weissman JS (2011) Ribosome profiling of mouse embryonic stem cells reveals the complexity and dynamics of mammalian proteomes. Cell 4:789–802

Kent OA, MacMillan AM (2004) RNAi: running interference for the cell. Org Biomol Chem 2:1957–1961

Lavorgna G, Dahary D, Lehner B, Sorek R, Sanderson CM, Casari G (2004) In search of antisense. Trends Biochem Sci 29:88–94

Mohammad F, Mondal T, Kanduri C (2009) Epigenetics of imprinted long noncoding RNAs. Epigenetics 4:277–286

Monk D, Sanches R, Arnaud P, Apostolidou S, Hills FA, Abu-Amero S, Murrell A, Friess H, Reik W, Stanier P, Constância M, Moore GE (2006) Imprinting of *IGF2* P0 transcript and novel alternatively spliced *INS-IGF2* isoforms show differences between mouse and human. Hum Mol Genet 15:1259–1269

Moore T, Constância M, Zubair M, Bailleul B, Feil R, Sasaki H, Reik W (1997) Multiple imprinted sense and antisense transcripts, differential methylation and tandem repeats in a putative imprinting control region upstream of mouse *Igf2*. Proc Natl Acad Sci USA 94:12509–12514

Okutsu T, Kuroiwa Y, Kagitani F, Kai M, Aisaka K, Tsutsumi O, Kaneko Y, Yokomori K, Surani MA, Kohda T, Kaneko-Ishino T, Ishino F (2000) Expression and imprinting status of human PEG8/IGF2AS, a paternally expressed antisense transcript from the *IGF2* locus, in Wilms' tumors. J Biochem 127:475–483

Pauler FM, Koerner MV, Barlow DP (2007) Silencing by imprinted noncoding RNAs: is transcription the answer? Trends Genet 23:284–292

Reik W, Walter J (2001) Genomic imprinting: parental influence on the genome. Nat Rev Genet 2:21–32

Rivkin M, Rosen KM, Villa-Komaroff L (1993) Identification of an antisense transcript from the IGF-II locus in mouse. Mol Reprod Dev 35:394–397

Taylor ER, Seleiro EA, Brickell PM (1991) Identification of antisense transcripts of the chicken insulin-like growth factor-II gene. J Mol Endocrinol 7:145–154

Wang KC, Chang HY (2011) Molecular mechanisms of long noncoding RNAs. Mol Cell 43:904–914

Wang Q, Carmichael GG (2004) Effects of length and location on the cellular response to double-stranded RNA. Microbiol Mol Biol Rev 68:432–452